J. Membrane Biol. 208, 141–153 (2005)
DOI: 10.1007/s00232-005-0825-9

The Journal of
Membrane
Biology

Optical Imaging and Functional Characterization of the Transverse Tubular System of Mammalian Muscle Fibers using the Potentiometric Indicator di-8-ANEPPS

M. DiFranco[1], **J. Capote**[1], **J.L. Vergara**[1,2]
[1]Department of Physiology, David Geffen School of Medicine, UCLA, Los Angeles, CA 90095, USA
[2]Department of Physiology, UCLA School of Medicine, 10833 Le Conte Avenue 53-263 CHS, Los Angeles, CA 90095-1751, USA

Received: 12 December 2005

Abstract. Potentiometric dyes are useful tools for studying membrane potential changes from compartments inaccessible to direct electrical recordings. In the past, we have combined electrophysiological and optical techniques to investigate, by using absorbance and fluorescence potentiometric dyes, the electrical properties of the transverse tubular system in amphibian skeletal muscle fibers. In this paper we expand on recent observations using the fluorescent potentiometric indicator di-8-ANEPPS to investigate structural and functional properties of the transverse tubular system in mammalian skeletal muscle fibers. Two-photon laser scanning confocal fluorescence images of live muscle fibers suggest that the distance between consecutive rows of transverse tubules flanking the Z-lines remains relatively constant in muscle fibers stretched to attain sarcomere lengths of up to 3.5 μm. Furthermore, the combined use of two-microelectrode electrophysiological techniques with microscopic fluorescence spectroscopy and imaging allowed us to compare the spectral properties of di-8-ANEPPS fluorescence in fibers at rest, with those of fluorescence transients recorded in stimulated fibers. We found that although the indicator has excitation and emission peaks at 470 and 588 nm, respectively, fluorescence transients display optimal fractional changes (13%/100 mV) when using filters to select excitation wavelengths in the 530–550 nm band and emissions beyond 590 nm. Under these conditions, results from tetanically stimulated fibers and from voltage-clamp experiments suggest strongly that, although the kinetics of di-8-ANEPPS transients in mammalian fibers are very rapid and approximate those of the surface membrane electrical recordings, they arise from the transverse tubular system membranes.

Key words: Fluorescent potentiometric indicators — Mammalian skeletal muscle — Transverse tubular system — Two-photon confocal imaging — Action potential — Sarcomere length — Potentiometric transients — Tetanic stimulation — Voltage clamp — Di-8-ANEPPS

Introduction

The vital role that the transverse tubular system (T-system) plays in skeletal muscle excitation-contraction (EC) coupling has been recognized since the pioneering experiments of Huxley and Taylor demonstrating that localized current stimulation in amphibian muscle fibers elicited sarcomeric contraction only when the stimulation pipette was placed at Z-lines where the T-tubules' openings are found (Huxley & Taylor, 1958). Compelling evidence, also obtained in amphibian muscle fibers, further suggested that the T-system is an active network with a sodium conductance contributing to the radial propagation of the action potential towards the center of the fiber (Adrian, Costantin & Peachey, 1969; Gonzalez-Serratos, 1971; Bezanilla et al., 1972; Adrian & Peachey, 1973; Bastian & Nakajima, 1974). Since the transmembrane potential of the T-tubules cannot be measured directly by electrical methods, the experimental confirmation of the existence of the so-called "T-tubular action potential" took years of painstaking effort involving the application of optical methods to muscle research. The endeavor was spearheaded by the development of dye molecules capable of staining biological membranes and of reporting fast changes (within a few microseconds) in

Correspondence to: J.L. Vergara; email: jvergara@mednet.ucla.edu

their transmembrane potentials (Salzberg, Davila & Cohen, 1973; Cohen et al., 1974; Ross et al., 1977). The first evidence showing rapid potentiometric dye fluorescence transients in frog skeletal muscles (Vergara & Bezanilla, 1976), although crucial for the future characterization of the electrical properties of the T-system, only suggested the existence of a T-tubular action potential (AP). Confirmation came later from single-fiber experiments where the use of more sophisticated electrophysiological methodology permitted independent electrical measurements of the surface membrane potential and optical measurements of the T-system's electrical activity (Nakajima & Gilai, 1980a, b; Vergara & Bezanilla, 1981; Heiny & Vergara, 1982).

Our investigation of the electrical properties of the T-system (Heiny & Vergara, 1982, 1984; Vergara et al., 1983; Heiny, Ashcroft & Vergara, 1983; Ashcroft, Heiny & Vergara, 1985; Vergara & Delay, 1986) was boosted by the development of highly fluorescent electrochromic indicators such as di-8-ANEPPS (Bedlack, Wei & Loew, 1992; Tsau et al., 1996; Obaid et al., 1999). Using this tool, we were able to demonstrate that supercharging command pulses (Armstrong & Chow, 1987) could be used to establish rapidly (within ~2 ms) voltage steps in the T-system (Kim & Vergara, 1998a, b) and to accelerate significantly the charge movement and calcium release from the sarcoplasmic reticulum (SB) (Kim & Vergara, 1998a). Nevertheless, in spite of this progress in characterizing the function properties of the amphibian T-system, a comparable description for the mammalian T-system was lacking. This was mostly due to limitations encountered in dissecting intact single mammalian fibers and mounting them in sophisticated electrophysiological/optical experimenta1 setups. However, recent advances in several laboratories, including ours, have demonstrated the feasibility of performing these kinds of studies in enzymatically dissociated muscle fibers (Head, 1993; Szentesi et al., 1997; Tutdibi et al., 1999; Woods et al., 2004, 2005). Using these methods, we have recently demonstrated that, unlike what was found in frog, in mouse *flexor digitorum brevis* (FDB) muscle fibers the time course of T-system optical signals elicited by action potentials and voltage pulses are almost undistinguishable from those at the surface membrane (Woods et al., 2005). These results are intriguing and deserving of further investigation. In the current studies we illustrate the advantages of using di-8-ANEPPS for the structural characterization of the T-system in live mammalian muscle fibers with two-photon laser scanning confocal microscopy (TPLSCM). Furthermore, we show new data and improved detection of di-8-ANEPPS fluorescence transients in mammalian muscle fibers, which give full support to the notion that, in spite of the rapid kinetics of the fluorescence signals, they originate in the T-system.

Materials and Methods

Biological Preparation

All experiments were carried out according to the guidelines laid out by the local UCLA Animal Care Committee. Muscle fibers from FDB and *flexor digitorum digiti quinti* (FDQ) muscles were enzymatically dissociated as described previously (Woods et al., 2004) except that 500 units/ml of collagenase IV (Worthington) were used, and transferred to custom-made, disposable, optical chambers. The chambers consisted of 35 mm plastic Petri dishes (Falcon 35–1008) with a circular cut at the center (16 mm in diameter) and sealed at the bottom with 18 × 18 mm microscope coverslips #1 glued on the external rim. FDB fibers were used at their slack length, while FDQ fibers were stretched to various lengths following the procedures described below.

Stretching of Dissociated Muscle Fibers

In experiments describing the effects of fiber stretching on the T-tubule structural organization, FDQ fibers (~10 mm in length) were held in place between strings of vacuum grease (*Glisseal*; Atomergic, Farmingdale, NY). The coverslips in this case were previously treated with a silanizing reagent (DiFranco et al., 1999). Two shallow strings of *Glisseal*, separated by a gap of ~100 μm, were laid on a dry coverslip. The chamber was then flooded with a solution consisting of fetal bovine serum (FBS, HyClon, Logan, UT) and Tyrode (1:1 v/v), and a few fibers transferred to it. Using fine fire-polished glass rods, the fibers were aligned across the gap and covered with *Glisseal* along their entire length, except for the gap section. The *Glisseal* on the two ends was then pulled away from the center gap to a variable extent so that, by carrying the ends of the fiber embedded in the grease, varying degrees of stretch were attained. Maximal stretching was obtained when the fibers started sliding out of the grease seals.

Once the fibers were mounted, the excess solution above the fibers was removed and another coverslip was laid flat at the air-liquid interface in order to assemble a fully enclosed chamber.

Solutions

The composition (in millimolar) of the solutions used in the experiments was as follows:

Tyrode solution: 150 NaCl, 10 MOPS, 2 $CaCl_2$, 10 dextrose, 1 $MgCl_2$, 2.5 KCl.

Tyrode TEA_2-SO_4: 182 TEA-OH, 15 MOPS, 5 CsOH, 3.25 $Ca(OH)_2$, 5 dextrose, 200 nM TTX, pH adjusted with H_2SO_4.

K-internal solution: 110 aspartic acid, 20 MOPS, 20 EGTA, 5 ATP-Mg, 5 Na_2 creatine phosphate, 3 reduced glutathione, 5 $MgCl_2$, 5 dextrose, 0.1 mg/ml CPK; pH adjusted with KOH.

Cs-internal solution: 78 Aspartic acid, 20 MOPS, 40 EGTA, 5 ATP-Mg, 5 di-TRIS creatine phosphate, 3 reduced glutathione, 20 $Ca(OH)_2$, 5 dextrose, 5 CsCl, 0.1 mg/ml CPK; pH adjusted with CsOH.

All solutions were adjusted to pH 7.2 and 300 mOsmol/kg H_2O. High EGTA concentrations in the internal solutions were used to prevent fiber contraction and potential movement artifacts in the optical records. Unless otherwise stated, the experiments were done at room temperature (20°C).

Electrophysiology

The electrical properties of FDB muscle fibers were studied under both current and voltage-clamp conditions using a two-microelectrode high-voltage amplifier (TEV-200, Dagan), as previously de-

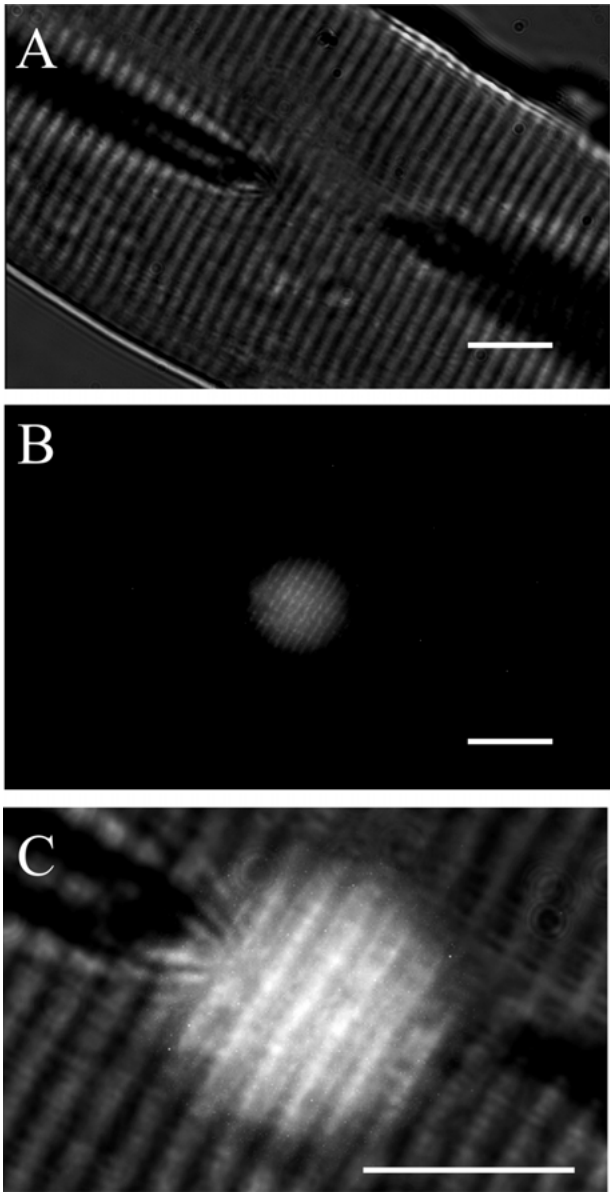

Fig. 1. Configuration for electrophysiological and optical measurements in isolated FDB fibers. Panel *A*. Brightfield image of an FDB fiber showing the relative impalement position of the voltage (*left*) and current (*right*) microelectrodes. Panel *B*. Fluorescence image of the illumination spot. Note the banded pattern corresponding to T-tubules stained with di-8-ANEPPS. Panel *C*. Enlarged view of the superposition of images in *A* and *B*. Note that the illumination spot is centered with respect to the microelectrodes' positions. Scale bars represent 10 μm for each image.

scribed (Woods et al., 2004, 2005). The typical microelectrode arrangement in an FDB fiber is shown in Fig. 1, panel *A*. As shown, the tips of the microelectrodes are placed approximately 10 μm apart along the midline of the muscle fiber.

In order to increase the frequency response of the microelectrodes, they were drawn to the largest tip size possible, compatible with the intact preservation of the muscle fibers. The voltage-recording electrodes had tip resistances in the 10–12 MΩ range, when filled with 3M KCl or 2 M K-Acetate. The current electrode, used to inject current and to load the cell with its content, had a resistance of 15–20 MΩ when filled with internal solutions. The electrodes' capacitance was maximally compensated with a positive feedback circuit (TEV-200, Dagan). Unless otherwise stated, the membrane potential of the fibers was adjusted to −90 mV in both current- and voltage-clamp conditions. In current clamp, action potentials were elicited by 0.5 ms rectangular pulses. In voltage clamp, the phase-adjustment control of the TEV-200 amplifier was tuned to avoid oscillations while attaining maximal feedback gain and speed. In some cases a pulse-subtracting (P/-2) protocol was used to remove linear resistive and capacitive currents. Voltage and current signals were filtered at 10 kHz.

Fiber Staining

Approximately 3 μg of di-8-ANEPPS (Invitrogen, Calabasas, CA) was dissolved in 2 μl of a solution of 10% Pluronic in DMSO (w/v). This solution was mixed with 10 ml of warm Tyrode solution (∼50°C) and sonicated for ∼30 seconds. Both types of muscle fibers were stained at room temperature (20°C) in the dye-Tyrode solution for 30–45 min, and washed thereafter with Tyrode.

Two-Photon Laser Scanning Confocal Microscopy

Optical chambers containing either slack or stretched muscle fibers were placed on the stage of an upright microscope (BX51WI, Olympus, Japan) equipped with an adjustable wavelength Chameleon Ti/Sapphire laser system (Coherent) and a Radiance 2000 Scanning Head (Bio-Rad, UK). Di-8-ANEPPS was excited at 920 nm (Fisher, Salzberg & Yodh, 2005) and its fluorescence detected through a 495//580–630 (dichroic//band-pass) emission filter combination. TPLSCM images were obtained with either a 20×, 0.95 NA (Olympus XLUMPLANFL) water-immersion objective (FDB fibers), or a 100×, 1.4 NA oil-immersion objective (FDQ fibers). In the latter case, the chamber was inverted and the fibers imaged through the coverslip glued to the bottom of the chamber. Image stacks were constructed from TPLSCM sections at focal planes separated every 1 μm in the *z*-axis of the microscope. Confocal image sections were analyzed using commercial (LaserSharp 2000, BioRad, UK) and/or public-domain image analysis software packages (Confocal Assistant and ImageJ).

From TPLSCM images of muscle fibers stained with di-8-ANEPPS, average fluorescence profiles were obtained from rectangular areas measuring at least 20 sarcomeres in length and at least 5 μm in width. These profiles were fitted with Gaussian distributions in order to determine the average spacing between consecutive T-tubules and the sarcomere length (*SL*) of the muscle fibers. The data is presented as mean ± standard error of the mean (SEM).

Detection of di-8-ANEPPS Fluorescence Signals

Stained FDB fibers were transferred to an optical chamber placed on the stage of an inverted microscope (IX-70, Olympus, Japan) equipped with a standard epifluorescence attachment and a 100W Hg illuminator. Fibers were imaged with an oil-immersion objective (100× 1.4 NA, Olympus). Several combinations of excitation filter//dichroic mirror//emission filter were used to excite the di-8-ANEPPS molecules staining the muscle fibers and to collect their fluorescence emission. A field diaphragm allowed for adjustment of the diameter of the illumination spot on the muscle fiber down to ∼5 μm; however, in the majority of the experiments the spot was set to 10–15 μm in diameter. Figure 1 shows the size of the illumination/fluorescence spot (∼10 μm in this case, panel *B*) and its relative position with respect to the

voltage and current microelectrodes (panel *C*). This localized configuration of the optical detection area assured that fluorescence signals were mostly recorded from regions of the muscle fiber where electrical measurements were recorded. The fluorescence emission from the area of illumination was focused on a PIN photodiode (PIN-HR008, United Detector Technology, Hawthorne, CA) connected to the headstage of a patch-clamp amplifier (Axopatch 1A, Axon Instruments). The photocurrent was filtered at 5 kHz. The fluorescence transients were normalized with respect to the resting fluorescence in $\Delta F/F$ units.

In Vivo Spectral Analysis of di-8-ANEPPS Fluorescence

An optical chamber with muscle fibers stained with di-8-ANEPPS was placed on the stage of an inverted fluorescence microscope (as above), but equipped with a fluorescence spectrum analyzer (EPP2000-HR, StellarNet, Tampa, FL). A disc-shaped region of the muscle fiber was imaged using the 100× 1.4 NA objective and a fluorescence cube with a band-pass excitation filter (460–480 nm), a dichroic mirror (500 nm), and a barrier filter (505LP). The fluorescence emission was focused directly onto one end of a fiber optic (Ø = 400 μm) placed at the image plane of an exit port of the microscope. The other end of the fiber optic was focused onto the imaging sensor of the spectrum analyzer. Fluorescence spectra were acquired continuously during integration times that ranged from 10–100 ms while the fiber was illuminated for variable duration intervals, as determined by the opening of a shutter under computer control.

Results

TPLSCM Imaging and Sarcomere-Length Dependence of the T-System Structural Organization

Vital staining of mammalian skeletal muscle fibers with di-8-ANEPPS, used in conjunction with high-resolution TPLSCM, allows for the study of the T-system organization in live fibers. Figure 2*A* and *C* presents images from a single *z*-axis plane of two FDQ fibers stretched to different lengths. The parallel bands of high fluorescence intensity in the TPLSCM images, which run perpendicular to the sarcolemma in the focal planes of Fig. 2*A* and *C*, correspond to di-8 ANEPPS staining of the T-tubules. It can be observed that these membrane structures are organized in the characteristic double row-per-sarcomere pattern of mammalian skeletal muscle fibres (Lannergren, Bruton & Westerblad, 1999; Woods et al., 2005) that results from the alignment of triads (T-tubule-sarcoplasmic reticulum junctions) within the sarcomere in pairs flanking the Z-line at the I bands (Revel, 1962; Franzini-Armstrong, Ferguson & Champ, 1988). We used TPLSCM image sections, like those shown in Fig. 2*A* and *C*, to obtain quantitative information about the effects of stretching on the spacing between consecutive T-tubules. The average fluorescence profile shown in Fig. 2*B* was obtained from a moderately stretched fiber (panel *A*) and yields an *SL* value (distance between equivalent peaks and valleys in the profile) of 2.54 ± 0.01 μm. In addition, the figure illustrates that there are two distinct distances between consecutive T-tubules: their separation flanking the Z-line (we call it TS_Z), and their separation across the M-line (we call it TS_M). For this fiber (Fig. 2*A* and *B*), TS_Z and TS_M were 0.81 ± 0.02 μm and 1.73 ± 0.01, respectively. In comparison, the highly stretched fiber of Fig. 2*C* yields an average fluorescence profile (Fig. 2*D*) with peaks and valleys significantly more separated. The following values for *SL*, TS_Z and TS_M respectively, were obtained: 3.18 ± 0.02, 1.03 ± 0.01 and 2.15 ± 0.02 μm. It can be readily verified that (within the statistical error) $SL = TS_Z + TS_M$ in both fibers.

The comparison of results such as those shown in Fig. 2*A* to *D*, make it apparent that increases in the *SL*, resulting from moderate and high stretches of the muscle fibers, respectively were accompanied by a substantial increase in TS_M but, perhaps also by an increase in TS_Z. We investigated this question thoroughly by generating fluorescence profiles in a population of fibers stretched at several lengths, and calculated the experimental values of *SL*, TS_Z and TS_M as described above. The resulting data was used to construct scatter-plots correlating TS_M with the *SL* (Fig. 2*E*) and TS_Z with the *SL* (Fig. 2*F*). The linear regression fitted to the data in Fig. 2*E* has a slope of 0.86 and demonstrates a strong correlation ($R = 0.98$; $P < 0.001$) between the degree of stretching of the muscle fiber and the separation of T-tubules across the M-line. In contrast, Fig. 2*F* demonstrates that there is almost no correlation between TS_Z and *SL*, as evidenced by a fitted regression line with a slope of 0.11 and $R = 0.47$ ($P > 0.1$). Put together, the experimental evidence obtained with TPLSCM and di-8-ANEPPS staining of the T-tubules suggests that stretching live mammalian skeletal muscle fibers results in the separation of consecutive Z-lines (increased *SL*) while they remain flanked by T-tubules at a comparatively constant distance. In other words, most of the increase in *SL* observed while stretching mammalian fibers occurs at the expense of increasing the length of the sarcomere segment centered at the M-line. Interestingly, this is where the majority of the contractile proteins are found (Squire, 1997).

Spectral Properties of di-8-ANEPPS AP Transients

Although the above image analysis shows that structural features of the T-system can accurately be investigated using di-8-ANEPPS, perhaps the most important feature of this fluorescent indicator is the ability to report on the functional properties of this membrane system by undergoing voltage-dependent

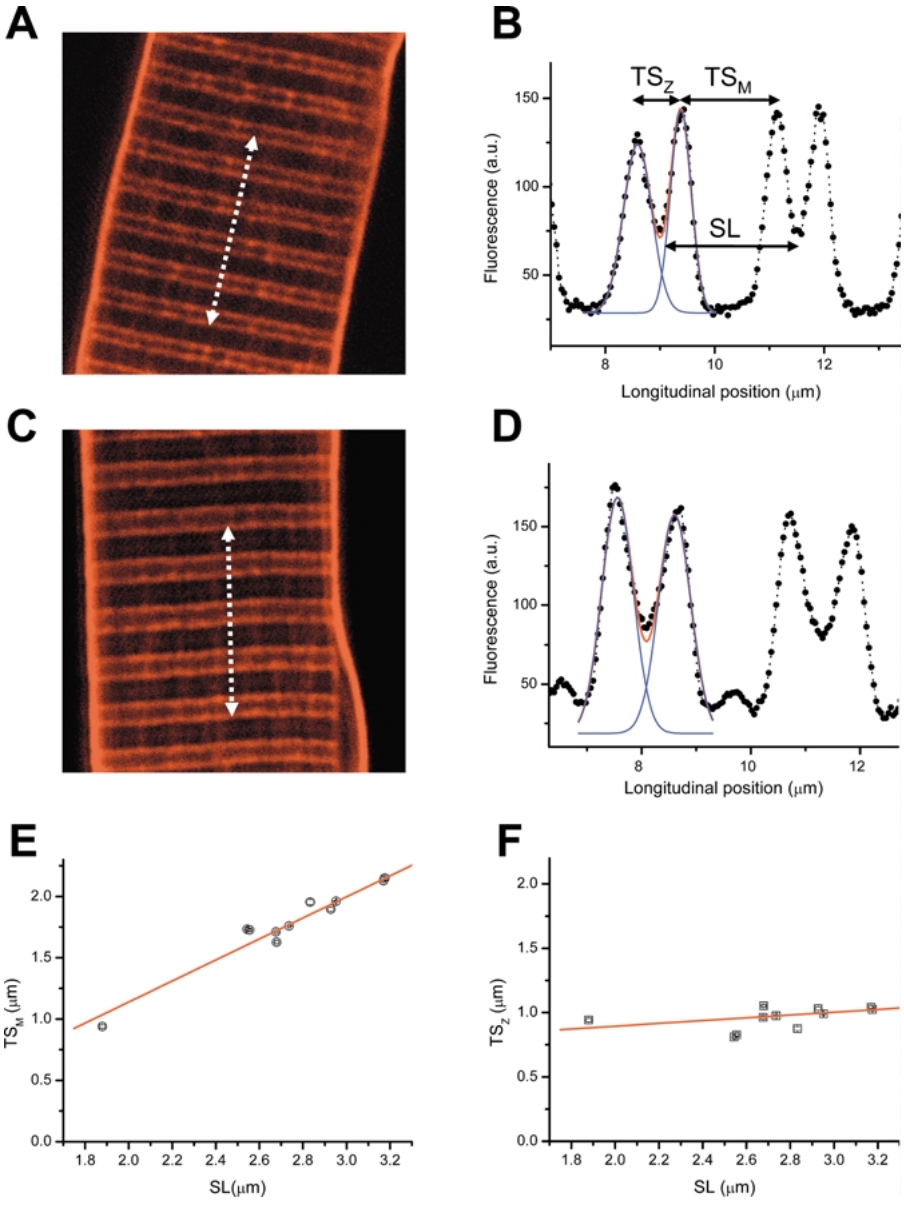

Fig. 2. Effects of fiber stretching on T-tubule spacing. Panels *A* and *C* are high magnification TPLSCM fluorescence images of FDQ fibers stained with di-8-ANEPPS and stretched to sarcomere lengths of 2.5 and 3.2 μm, respectively. Double headed arrows represent 12.5 and 12.8 μm for panels *A* and *C*, respectively. Panels *B* and *D*. Longitudinal intensity profiles from the fibers in panels *A* and *C*, respectively. Measurements were made in rectangular areas (5 μm wide and 20 sarcomeres in length) along the direction indicated by the double headed arrows. TS_Z is the distance between consecutive T-tubules flanking each M-line. TS_M is the distance between consecutive T-tubules at both sides of each M-line. *SL* is the sarcomere length. The fluorescence peaks were fitted with Gaussian curves (*blue traces*) and each pair of fluorescence peaks separated by TS_Z was fitted with double Gaussian. Panels *E* and *F*. Dependence of TS_M (*E*) and TS_Z (*F*) on the sarcomere length. The straight lines are linear fits to the data. External solution: Tyrode.

changes in its spectral properties (Rohr & Salzberg, 1994; Kim & Vergara, 1998a, b; Zhang et al., 1998; Obaid et al., 1999). In this regard, we wanted to investigate further the spectral properties of di-8-ANEPPS staining the T-system membranes of mammalian fibers at rest, and later compare them with those of fluorescence transients associated with AP stimulation of the muscle fibers. Figure 3*A* (*continuous trace*) shows the emission spectrum of di-8-ANEPPPS recorded from a quiescent FDD muscle fiber (membrane potential = −90 mV). It should be noted that this emission spectrum, obtained while using the optimal excitation wavelengths of the indicator (460–480 nm), is significantly narrower -and blue-shifted (full-width-at-half-maximum [FWHM] = 84 nm; peak at 588 nm) compared with that reported for stained liposomes by the dye manufacturer (Molecular Probes, Invitrogen; FWHM = 152 nm; peak at 628 nm). These spectral discrepancies, though important, probably arise from intrinsic differences in lipidic composition of the membranes where the dye molecules are embedded (Gross, Bedlack & Loew, 1994). We then recorded simultaneously APs and their corresponding T-system fluorescence transients using the same excitation filter and dichroic mirror as for the spectrum (460–480//505 nm; *see* Methods), but with several long-pass filters ranging from 540LP to 645LP. Figure 3*B* shows di-8-ANEPPS transients recorded with 540LP (smaller-amplitude trace) and 645LP (larger-amplitude trace); Fig. 3*C* shows the corresponding APs. It can be observed that the membrane depolarizations during the APs are associated with rapid transient fluorescence decreases that are larger in amplitude at 645LP than at 540LP ((Δ*F*/

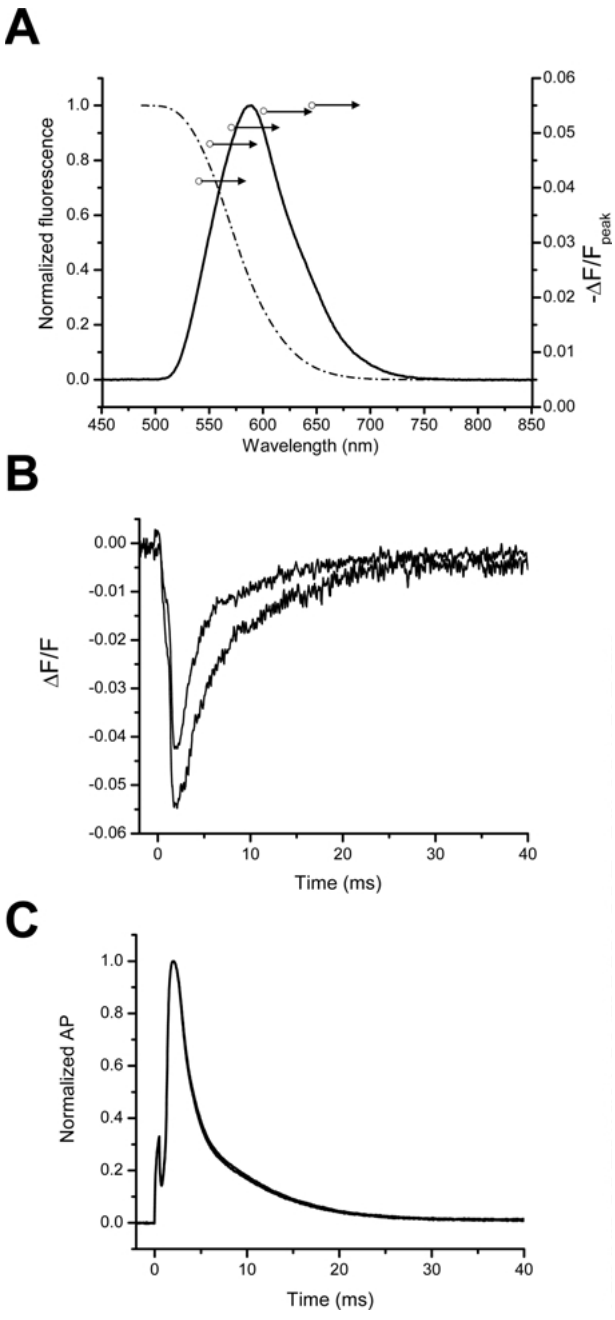

Fig. 3. In vivo spectral analysis of di-8-ANEPPS fluorescence emission. Panel *A*. The continuous line is the emission spectrum of di-8-ANEPPS staining the T-tubules of an FDB fiber. The *circles* represent the negative of the maximal $\Delta F/F$ ($-\Delta F/F_{peak}$) of fluorescence transients detected with 450LP, 550LP, 570LP, 600LP and 645LP long-pass filters. They were plotted as a function of the cut-on wavelength of each filter. The dotted line represents the complementary integral of the di-8-ANEPPS spectrum ($1 - \int$*emission spectrum*). Panel *B*. Single-sweep recordings of fluorescence changes associated with AP stimulation of the muscle fiber. The largest and smallest transients depicted in the figure were obtained using 540LP and 645LP filters, respectively. Panel *C*. Superposition of APs corresponding to traces in *B*. External solution: Tyrode. Internal solution: K-internal.

$F)_{peak} = -0.055$ and -0.043, respectively). The amplitudes of the di-8-ANEPPS transients were plotted as a function of the cut-on wavelength of the filter and superimposed (changing their sign for comparison) with the dye's emission spectrum (*empty circles* in Fig. 3*A*). It can be observed that the amplitude of the transients increases monotonically with the cut-on wavelength, which is contrary to the expectation if the T-tubule signals represented changes in quantum yield while the fluorescence spectral properties of the dye in the resting fiber were preserved. In the latter case, the transients' amplitude should have displayed a wavelength dependence comparable to that of the complementary integral of the emission spectrum as shown in Fig. 3A (*dotted line*).

We investigated the spectral properties of di-8-ANEPPS fluorescence transients further by considering two scenarios. The first one was that, as suggested by Fig. 3*A*, reducing the width and cut-on wavelength of the emission filter should eventually report positive fluorescence signals associated with APs. This set of conditions was implemented by using a cube similar to those described above, but replacing the long-pass filter with a bandpass emission filter in the green region of the spectrum (513–557 nm). A typical record under these conditions is shown in Fig. 4*A* (positive $\Delta F/F$, *dotted trace*). The other scenario was to emulate the excitation/emission conditions that gave the largest transients in cultured heart cells (Rohr & Salzberg, 1994). To this end, we used a cube with the configuration 530–550//550//590LP and obtained records like the negative-going transient in Fig. 4*A* (negative $\Delta F/F$, *continuous trace*). Figure 4*B* demonstrates that positive and negative $\Delta F/F$ records were elicited by essential identical APs. Interestingly, the amplitude of the positive transient ($\Delta F/F \sim 0.08$) was comparable to the largest of the negative transients described above (Fig. 3*B*, emission 645LP); however, the negative-going transient has more than double the amplitude of the positive transient ($\Delta F/F \sim -0.18$). Fig. 4*C* demonstrates that when both signals are scaled and displayed superimposed in the positive direction they have almost identical time courses, except for a small negative inflection in the late phase of one of the traces (*continuous trace*). Although this negativity is not observed in all fibers (*see* below), discrepancies between optical records at different wavelengths are intriguing and deserving of further investigation. In any event, the results in mammalian fibers that will be presented in the rest of this paper were obtained with the more efficient cube configuration (530–550//550//590LP), but for convenience, the negative $\Delta F/F$ transients will be shown as upward deflections for depolarizing voltages.

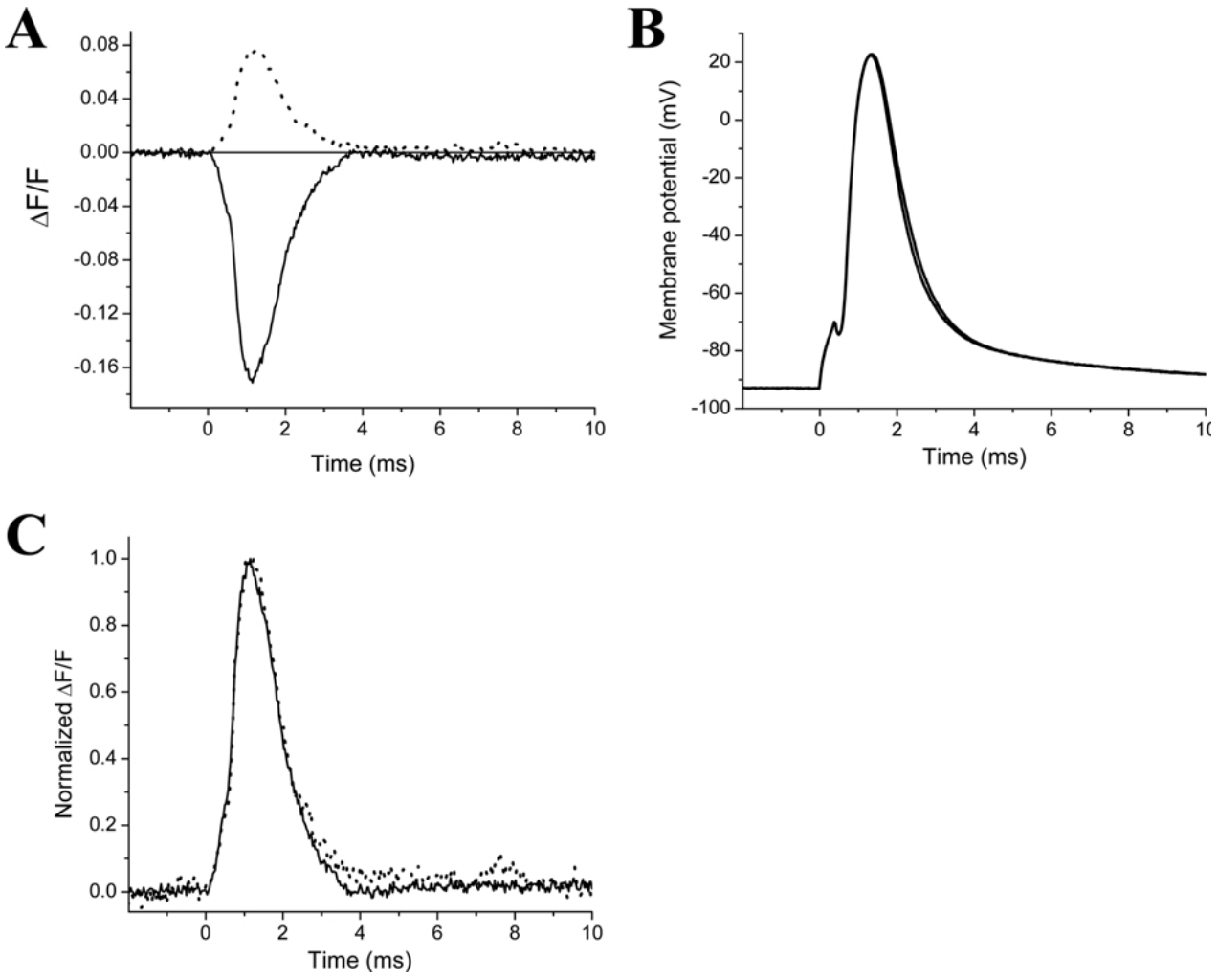

Fig. 4. "Green" and "red" di-8-ANEPPS transients. Panel *A*. Single-sweep fluorescence transients recorded from an FDB fiber stained with di-8-ANEPPS using a 460–500//500//513–557 cube (upward, "green") and a 530–550//550/590 cube (downward, "red"). Panel *B*. Superposition of APs corresponding to traces in *A*. Panel *C*. Superimposed display of normalized "green" and "red" transients. Fiber radius: 28 μm. External solution: Tyrode. Internal solution: K-internal.

Optical and Electrical Properties of T-System APs

We have recently reported that the time course of the di-8-ANEPPS fluorescence transient in mammalian muscle fibers matches closely that of the electrical recording of the surface AP (Woods et al., 2005). Figure 5*A* (left panel) illustrates this by showing the superposition of the AP and the fluorescence transient from an FDB fiber. In this case, the improved signal-to-noise (S/N) ratio of the optical transient ($\Delta F/F_{peak} = 0.18$; S/N = 15) leaves little doubt that, for a single AP, the kinetics of the T-system signal are very similar to those of the electrical record. This is in sharp contrast with what has been reported in frog skeletal muscle fibers (Kim & Vergara, 1998a, b) where the T-system transient has significantly slower rising and falling phases than the electrical AP, as illustrated in the right panel of Fig. 5*A*. It should be noted that discrepancies between optical records and electrically recorded APs are expected to be strongly influenced by the fiber radius (Adrian & Peachey, 1973; Ashcroft et al., 1985; Kim & Vergara, 1998b). Thus, it is not surprising that the kinetics of the di-8-ANEPPS transient from the thinner mammalian FDB fiber (radius, 27 μm) more closely approximate those of the AP than in the case of the thicker frog muscle fiber (radius, 60 μm). However, as noted previously (Woods et al., 2005), the similarity between electrical and optical signals in mammalian muscle fibers is almost too perfect, and this feature could raise concerns about the possibility that the T-system membrane potential may not be properly represented by the di-8-ANEPPS signals. Direct evidence that this is not the case is given in Fig. 5*B* and *C* and in the remainder of this paper.

Electrical and optical records from the same fiber in Fig. 5*A* (left panel), when stimulated at 100 and

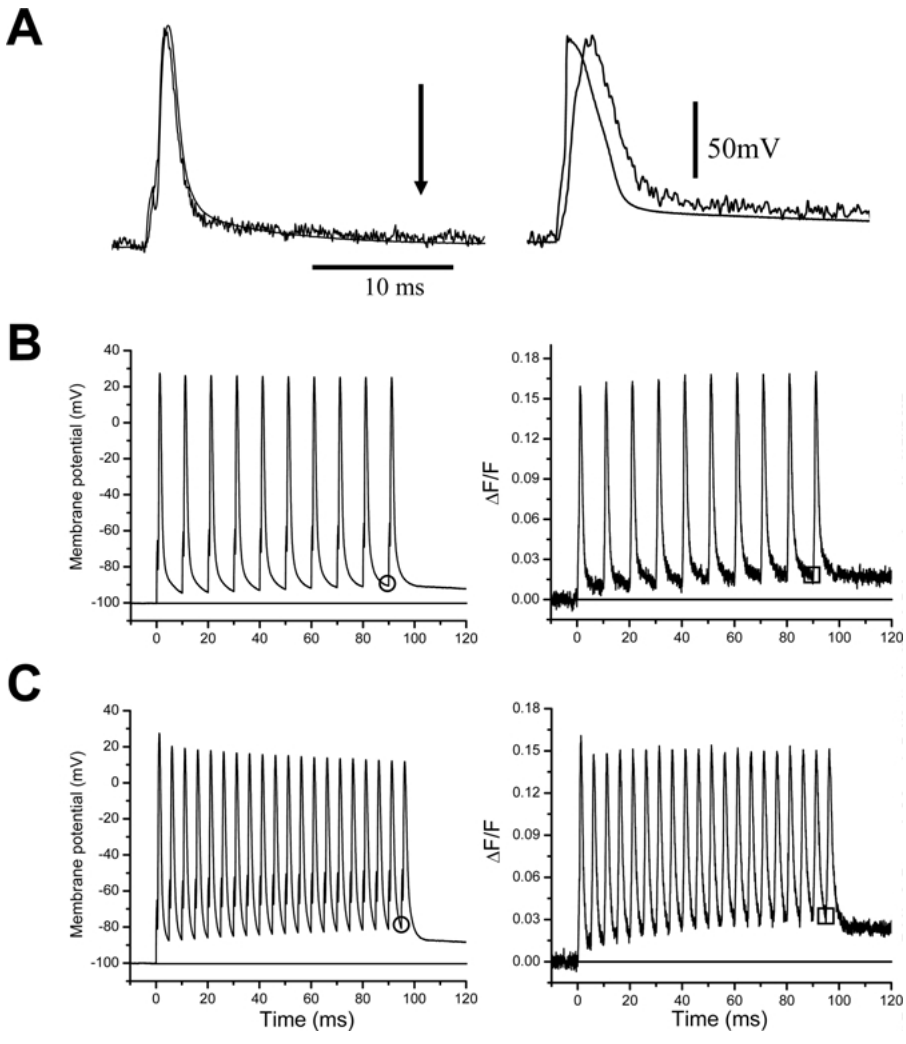

Fig. 5. Di-8-ANEPPS transients from mammalian and amphibian skeletal muscle fibers. Panel *A*. Superimposed di-8-ANEPPS and AP records from mouse (*right*) and frog (*left*) muscle fibers. Smooth and noisy traces are APs and fluorescence records, respectively. The arrow indicates the direction of $\Delta F/F$ increases and its length corresponds to 10% and 5.8% for the mouse and frog records, respectively. The frog records were obtained from a cut fiber preparation (Kim & Vergara, 1998a; Kim & Vergara, 1998b). Temperature: 20°C (mouse) and Panels *B* and *C*. Trains of APs (*right*) and fluorescence transients (*left*) elicited in response to current pulses delivered at 100 Hz (panel *B*) and 200 Hz (panel *C*). External solution: Tyrode. Internal solution: K-internal.

200 Hz tetanic frequencies, are shown in Fig. 5*B* and *C*, respectively. It can be observed that the response time of di-8-ANEPPS is rapid enough to track faithfully the fast voltage changes occurring at each AP during the tetanic trains. Nevertheless, the repolarization between consecutive APs is less complete in the di-8-ANEPPS records than in the electrical records. This limitation is more apparent late during the trains of APs and at higher frequencies of stimulation. For example, the membrane potential after the 9th AP (*circle* in left panel of Fig. 5*B*) was −90 mV, which represents 92.2% repolarization with respect to the value at the peak of the AP (+27 mV). The reciprocal point for the optical trace (*square* in right panel of Fig. 5*B*) has a $\Delta F/F$ value of 0.018, which represents 89.3% recovery from the peak $\Delta F/F$ value of 0.165 for that AP. For the 200 Hz tetanus in Fig. 5*C*, the recovery values after the 19th AP are 82.5% and 77.5% for the electrical and optical traces, respectively. This analysis, demonstrating that optical records progressively deviate from the electrically recorded voltage at higher frequencies and longer times, can be readily explained on the following basis: a) electrical and optical records predominantly monitor voltage changes across two different membrane compartments, surface and T-system, respectively; b) each membrane compartment is characterized by its own set of voltage-dependent conductances and passive electrical parameters; and c) voltage changes in the T-system are influenced by long-term use-dependent phenomena such as ion accumulation (or depletion) in the lumen of the T-tubules.

Changes in di-8-ANEPPS Fluorescence in Response to Step Changes in Membrane Potential under Voltage-Clamp Conditions

An important validation of the use of potentiometric indicators for measurements of potential changes in electrically inaccessible membrane compartments, such as the T-system in skeletal muscle fibers, is to demonstrate that optical signals vary linearly with voltage when all ionic conductances have been

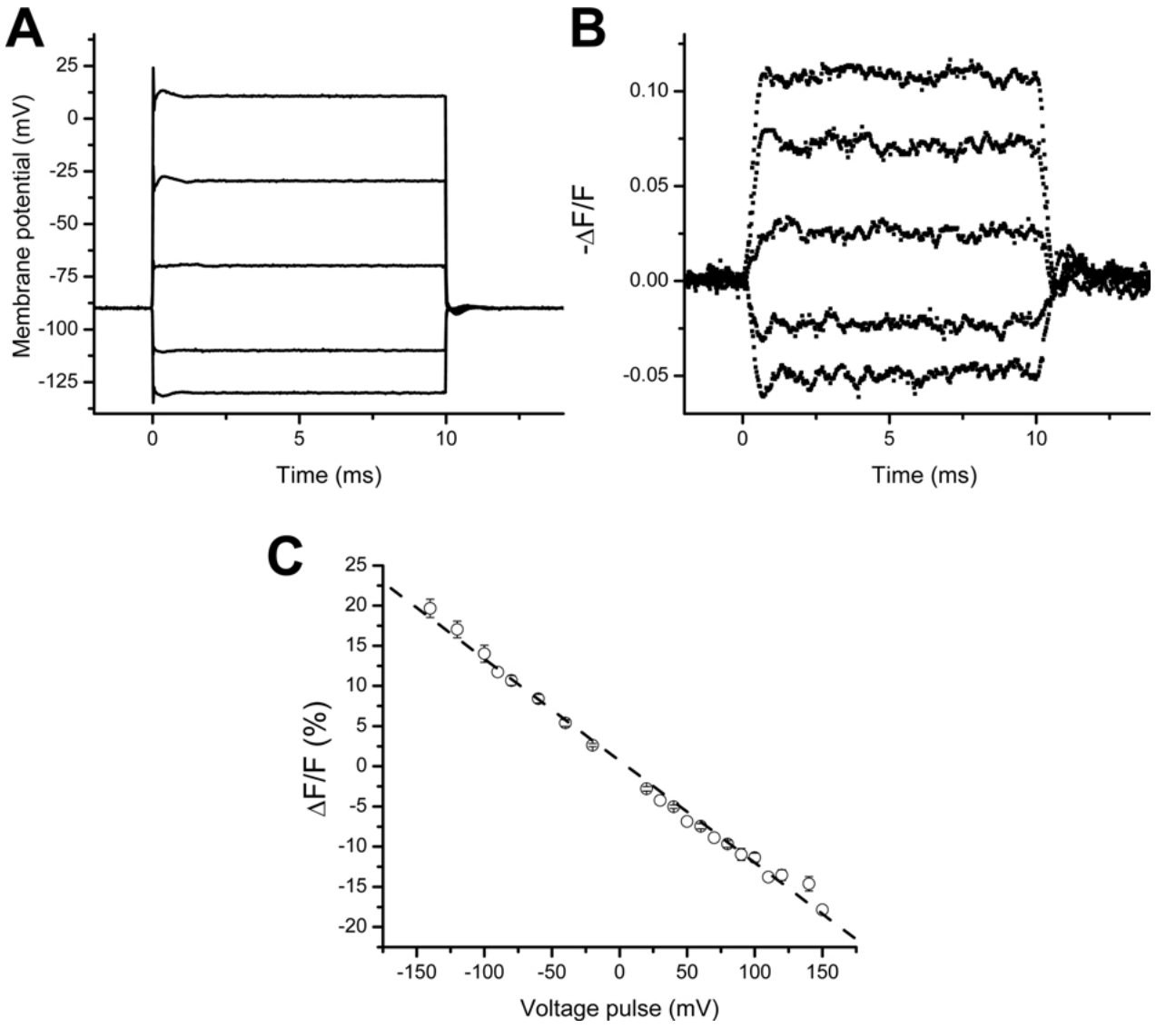

Fig. 6. Voltage dependence of di-8-ANEPPS fluorescence. Panel *A*. Membrane potential changes in response to 10 ms voltage steps of −20, −40, 20, 60 and 100 mV. The holding potential was −90 mV. Panel *B*. Di-8-ANEPPS transients recorded in response to the pulses in panel *A*. The signals are shown inverted to facilitate comparison with the voltage pulses. Fiber radius: 25 μm. Panel *C*. Steady state $\Delta F/F$ values plotted as a function of the magnitude of the voltage pulses. Data points (*circles* and *error bars*) are mean ± SEM from 3 fibers. The dotted line is a linear regression of the data (slope: 0.13; *y*-axis intercept: 0.69; $R = 0.996$). External solution: Tyrode TEA_2-SO_4. Internal solution: Cs-internal.

blocked. This test was performed previously in amphibian muscle fibers for the absorbance potentiometric indicator NK2367 (Heiny & Vergara, 1982) and for di-8-ANEPPS (Kim & Vergara, 1998b), and recently in mammalian muscle fibers for di-8-ANEPPS, using a 473–503//505//600LP fluorescence cube (Woods et al., 2005). We wanted to verify these latter observations using the more efficient illumination/detection protocols described above. FDB muscle fibers were rendered electrically passive by using ion replacement and conductance blockers (Cs-internal solution and Tyrode TEA_2-SO_4 external solution; *see* Methods). Figure 6 shows voltage records (panel *A*) and optical transients (panel *B*) recorded in response to step pulses 10 ms in duration. It can be observed that the T-system optical transients have a remarkable similarity to the voltage steps imposed at the surface membrane, except for the intrinsic noise and slightly slower rising and falling phases ($\tau \sim 0.3$ ms). In order characterize the voltage dependence of the di-8-ANEPPS signals, we plotted the steady-state fluorescence changes (expressed in $\Delta F/F$ % change) as a function of the pulse amplitude for a family of hyperpolarizing and depolarizing voltage-clamp pulses (applied from a holding potential of −90 mV). Pooled data from 3 fibers are shown

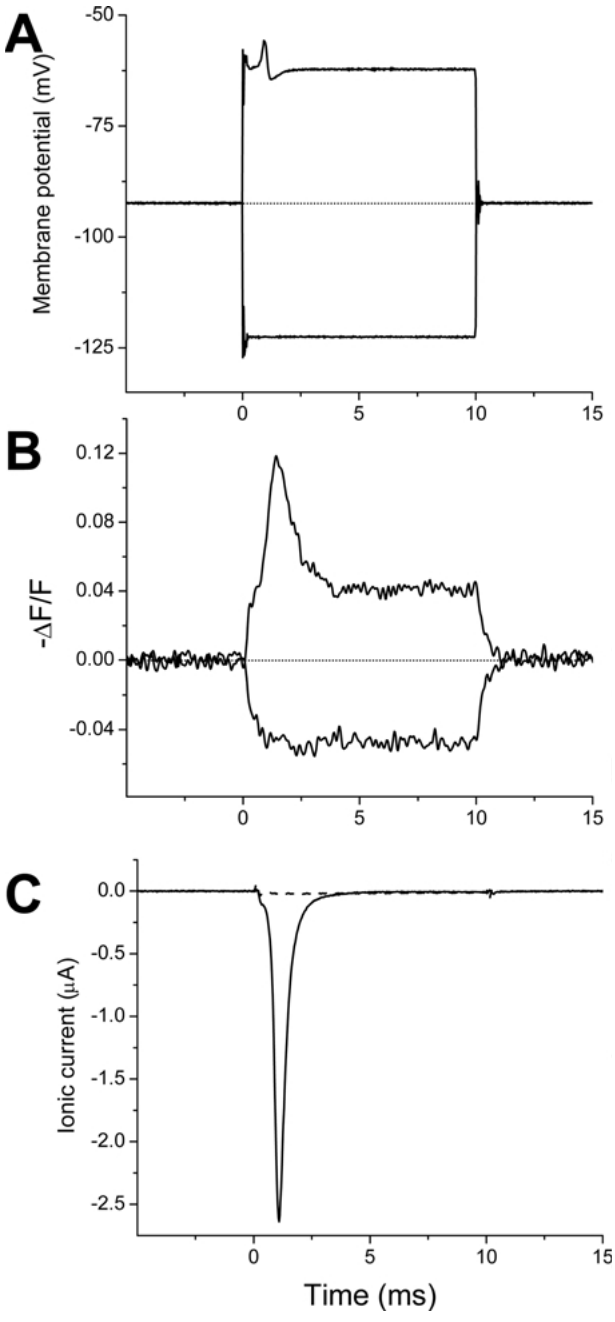

Fig. 7. Asymmetrical T-system records associated with equal amplitude hyperpolarizing and depolarizing voltage-clamp pulses in the presence of external Na^+. Panel *A*. Membrane potential records in response to 10 ms, ± 30 mV pulses applied from a holding potential of −90 mV. Panel *B*. Di-8-ANEPPS records associated with the pulses in *A*. Panel *C*. Ionic currents recorded in response to +30 mV (*continuous trace*) and −30 mV (*dashed trace*) voltage-clamp pulses. The current records were obtained using a P/-2 subtraction protocol in order to eliminate linear capacitative components. Fiber radius: 18 μm. External solution: Tyrode. Internal solution: K-internal.

in Fig. 6*C*. A slope of −13% $\Delta F/F$ per 100 mV was found from the linear regression fit to the data. With this information, we estimate that the amplitude of the T-system APs for the optical trace in the left panel of Fig. 5*A* is ∼123 mV, quite similar to the amplitude of the electrically recorded AP (124 mV).

Asymmetry in the T-System Signals Due to Sodium Current Activation

A useful strategy for highlighting differences in the electrical behavior of the surface membrane compared with that of the T-system in frog skeletal muscle fibers was to perform voltage-clamp experiments in the presence of external Na^+ and to demonstrate asymmetry between optical records obtained with hyperpolarizing and depolarizing pulses owing to the presence of Na^+ currents in the T-system, while the surface membrane is symmetrically polarized (Vergara & Bezanilla, 1981; Heiny & Vergara, 1982). Results from an experiment of this kind, but in a mammalian FDB muscle fiber stained with di-8-ANEPPS, are illustrated in Fig. 7. Figure 7*A* shows ±30 mV, 10 ms voltage-clamp steps used to stimulate a fiber immersed in Tyrode solution. It should be noted that, while the onset of the voltage step for both polarities was attained within the ∼50 μs settling time of the voltage-clamp circuit, the depolarizing pulse (upward record, Fig. 7*A*) displays a small transient deviation from the steady level (∼9 mV peak-to-peak), which is due to a relatively minor lack of membrane potential control (escape) resulting from the activation of the large Na^+ inward current (*continuous trace*, Fig. 7*C*). In contrast to the similarity between the positive and negative voltage pulses, the fluorescence records in Fig. 7*B* demonstrate significant asymmetries between the signals associated with hyperpolarizing (*downward trace*) and depolarizing (*upward trace*) pulses. In association with the −30 mV voltage pulse, the fluorescence record shows an exponential rise to a steady-state $\Delta F/F$ value of ∼0.05, followed by a monotonic decay to the resting level at the off of the pulse. Instead, the early phase of the depolarizing optical record rises to a large peak ($\Delta F/F = -0.12$), decays rapidly towards a steady value comparable to that observed during the hyperpolarizing pulse ($\Delta F/F = -0.045$), and then also decays monotonically at the off of the pulse. It should be noted that the $\Delta F/F$ peak observed during the depolarizing optical signal occurs ∼0.3 ms later than the inward current peak (Fig. 6*C*), suggesting a delayed temporal correlation between the activation of the Na^+ conductance at the surface membrane and the regenerative "escape of membrane potential control" in the T-system. Interestingly, using the ∼13%/100 mV regression value for the optical signals (*see* above), we calculate that the ∼2.7-fold asymmetry between the $\Delta F/F$ peak observed during the +30 mV pulse and the steady-state value during the −30 mV pulse corresponds to ∼80 mV asymmetry in the T-system potentials. This value exceeds by far the 9 mV ripple observed in the depolarizing voltage trace.

Discussion

In skeletal muscle, the T-system is a membrane compartment with a precise geometry likely to be crucial for the physiological role it plays in EC coupling. We investigated structural features of the T-system organization in mammalian skeletal muscle by means of the acquisition in vivo of TPLSCM images from FDB fibers stained with di-8-ANEPPS (Fig. 2). The di-8-ANEPPS fluorescence images showed a double row of T-tubules per sarcomere, a distinctive feature of mammalian skeletal muscle fibers that has been documented previously (Revel, 1962; Dulhunty, 1989; Franzini-Armstrong, Protasi & Ramesh, 1998; Lannergren et al., 1999). Furthermore, electron microscopical evidence has shown that in unstretched mammalian fibers the triads, structural assemblies consisting of one T-tubule and two sarcoplasmic reticulum (SR) terminal cisternae, are located at both sides of the Z-line in the I-A junction region of the sarcomere (Revel, 1962; Dulhunty, 1989; Franzini-Armstrong et al., 1998). Nevertheless, data about the sarcomeric localization of the T-tubules in stretched fibers is lacking. This information is crucial for the understanding of EC coupling mechanisms since the T-tubules, as the central elements of the triads that play a crucial role in the control of Ca^{2+} release, are ultimately responsible for the mechanical activation of the muscle fibers. Our findings that the distance between consecutive T-tubules remains essentially constant when the sarcomere is stretched to up to 3.5 μm suggest that the T-tubules are somehow anchored to structural components of the I band, perhaps the Z-line itself. A functional verification that this may be the case was provided by preliminary data demonstrating that Ca^{2+} release domains do not separate upon stretching of mammalian FDQ fibers (DiFranco et al., 2003).

Our results that the emission spectral properties of di-8-ANEPPS staining the T-system membranes of mammalian muscle fibers (Fig. 3*A*) differs from those in liposomes support the idea that the lipid environment is important in determining the dye's fluorescence (Gross et al., 1994), and are in line with findings that the lipidic composition of the T-tubules is atypical (Hidalgo, 1985; Pediconi et al., 1987). However, it is interesting that the spectral properties of T-system fluorescence signals seem to agree with results from a variety of biological preparations. For example, our results using illumination wavelengths centered in the excitation peak of the dye molecules (460–480 nm; Fig. 3) confirm evidence obtained for di-4-ANEPPS (Knisley et al., 2000) and di-8-ANEPPS (Rohr & Kucera, 1998) in heart muscles that membrane depolarizations can be detected as positive "green" signals (Fig. 4*A*, *dotted trace*) and negative "red" signals (Fig. 2*B*), depending upon the emission wavelengths chosen. Furthermore, we also verified the observations made in cultured cardiac cells by Rohr and Salzberg (1994) and by Obaid et al. in neurons (Obaid et al., 1999) that transients with optimal % $\Delta F/F$ change were obtained when the illumination wavelength was chosen in the green range of the spectrum (513–557 in our case) and the fluorescence collected in the red range (>590 nm). Under these conditions (Fig. 4*A*, *continuous trace*; Fig. 5*A*, *left panel*; Fig. 5*B* and *C*), we obtained values of fractional fluorescence change for di-8-ANEPPS transients in mammalian fibers that consistently approximated the 13%/100 mV given in Fig. 6. This value is close to the 10.3%/100 mV reported in cardiac cells (Rohr & Salzberg, 1994) and the 15%/100 mV neuroblastoma N1E-115 cells (Zhang et al., 1998), but larger than the 6%/100 mV previously reported by our laboratory, using other wavelength selections, in frog and mammalian muscle fibers (Kim & Vergara, 1998b; Woods et al., 2005). Most importantly, by using the 530–550//550//590LP (excitation//dichroic//emission) configuration we were able to record, from a very narrow illumination region of FDB muscle fibers (10–15 μm disc-shaped; Fig. 1) comprising a small number of T-tubules, AP-evoked transients with an S/N ratio of up to 25:1 in a single sweep (5 kHz bandwidth).

Altogether, the observed spectral properties of di-8-ANEPPS fluorescence signals in mammalian muscle fibers are compatible with the scheme, proposed for similar electrochromic indicators, that in response to membrane depolrizations, dye molecules may undergo voltage-induced electrochromic and solvation changes which potentially result in blue-shifts in their excitation spectrum, less prominent blue-shifts in their emission spectrum, and changes in their fluorescence quantum efficiency (Fromherz & Lambacher, 1991).

The excellent sectioning power of the 1.4 NA objective used in our experiments and this large T-system/surface membrane ratio of mammalian fibers (Eisenberg, 1983) strongly suggest that, as demonstrated extensively in frog muscle fibers (Vergara & Bezanilla, 1981; Heiny & Vergara, 1982, 1984; Kim & Vergara, 1998b), the fluorescence signals reported here originate essentially from the T-system. Nevertheless, the kinetic similarity between fluorescence and electrical signals, obtained both in current- and voltage-clamp conditions, prompted us to devise experiments capable of discriminating between the expected contributions from each membrane compartment (surface membrane and T-system). The first piece of evidence was obtained using tetanic stimulation (Fig. 5*B* and *C*). Although single AP records clearly demonstrate that di-8-ANEPPS faithfully tracks the electrical AP, trains of APs elicited at tetanic frequencies unveiled discrepancies between the optical and electrical signals. Since these differences manifested themselves relatively late

during the periods of repetitive stimulations, and they depended on the frequency of stimulation, it is unlikely that they reflect limitations in the optical probe or in the detection system. Instead, they probably arise from physiological processes endogenous to the T-system, such as ion accumulation (or depletion) in the lumen of the T-tubules. The importance of these findings is that such processes have been claimed, but never measured directly, in mammalian skeletal muscle fibers (Cannon, Brown & Corey, 1991; Cairns et al., 2003; Cairns, Ruzhynsky & Renaud, 2004).

More dramatic evidence was obtained under voltage-clamp conditions. When step voltage pulses of both signs were applied to fibers rendered electrically passive, both electrical and optical recordings showed symmetrical responses. Nevertheless, if the experiments were performed under conditions that permitted the activation of the sodium currents, a large asymmetry was seen in the optical records, while the electrical signals showed only a small artifact reflecting the brief voltage-clamp failure owing to the sodium current. It is important to recall that the optical records were obtained within a small region of the muscle fiber immediately adjacent to the voltage microelectrode; consequently, the asymmetrical behavior must arise from a membrane compartment not accessible to this electrode, namely the T-system. These results closely emulate observations made with other potentiometric indicators in amphibian muscle fibers (Vergara & Bezanilla, 1981; Heiny & Vergara, 1982). Most significantly, Na-dependent asymmetries are readily predicted by model simulations of the electrical propagation in the T-system (Ashcroft et al., 1985), provided that a voltage-dependent Na^+ conductance is included (Vergara et al., 1983).

This work was supported by National Institutes of Health grants AR47664 and GM074706, and a Grant in Aid from the Muscular Dystrophy Association.

References

Adrian, R.H., Costantin, L.L., Peachey, L.D. 1969. Radial spread of contraction in frog muscle fibres. *J. Physiol.* **204:**231–257

Adrian, R.H., Peachey, L.D. 1973. Reconstruction of the action potential of frog sartorius muscle. *J. Physiol.* **235:**103–131

Armstrong, C.M., Chow, R.H. 1987. Supercharging a method for improving patch-clamp performance. *Biophys. J.* **52:**133–136

Ashcroft, F.M., Heiny, J.A., Vergara, J. 1985. Inward rectification in the transverse tubular system of frog skeletal muscle studied with potentiometric dyes. *J. Physiol.* **359:**269–291

Bastian, J., Nakajima, S. 1974. Action potential in the transverse tubules and its role in the activation of skeletal muscle. *J. Gen. Physiol.* **63:**257–278

Bedlack, R.S. Jr., Wei, M., Loew, L.M. 1992. Localized membrane depolarizations and localized calcium influx during electric field-guided neurite growth. *Neuron* **9:**393–403

Bezanilla, F., Caputo, C., Gonzalez-Serratos, H., Venosa, R.A. 1972. Sodium dependence of the inward spread of activation in isolated twitch muscle fibres of the frog. *J. Physiol.* **223:**507–523

Cairns, S.P., Buller, S.J., Loiselle, D.S., Renaud, J.M. 2003. Changes of action potentials and force at lowered $[Na^+]_o$ in mouse skeletal muscle: implications for fatigue. *Am. J. Physiol.* **285:**C1131–C1141

Cairns, S.P., Ruzhynsky, V., Renaud, J.M. 2004. Protective role of extracellular chloride in fatigue of isolated mammalian skeletal muscle. *Am. J. Physiol.* **287:**C762–C770

Cannon, S.C., Brown, R.H. Jr., Corey, D.P. 1991. A sodium channel defect in hyperkalemic periodic paralysis: potassium-induced failure of inactivation. *Neuron* **6:**619–626

Cohen, L.B., Salzberg, B.M., Davila, H.V., Ross, W.N., Landowne, D., Waggoner, A.S., Wang, C.H. 1974. Changes in axon fluorescence during activity: molecular probes of membrane potential. *J. Membrane Biol.* **19:**l–36

DiFranco, M., Quinonez, M., DiGregorio, D.A., Kim, A.M., Pacheco, R., Vergara, J.L. 1999. Inverted double-gap isolation chamber for high-resolution calcium fluorimetry in skeletal muscle fibers. *Pfluegers Arch.* **438:**412–418

DiFranco, M., Woods, C.E., Novo, D., Vergara, J.L. 2003. Intrasarcomeric calcium release domains in enzymatically dissociated mouse skeletal muscle fibers. *Biophys. J.* **82:**641a

Dulhunty, A.F. 1989. Feet, bridges, and pillars in triad junctions of mammalian skeletal muscle: their possible relationship to calcium buffers in terminal cisternae and T-tubules and to excitation-contraction coupling. *J. Membrane Biol.* **109:**73–83

Eisenberg B.R. 1983. Chapter 3: Quantitative ultrastructure of mammalian skeletal muscle. In: L.D. Peachey, editor, Handbook of Physiology. pp. 73–112. American Physiological Society, Bethesda, MD

Fisher, J.A., Salzberg, B.M., Yodh, A.G. 2005. Near infrared two-photon excitation cross-sections of voltage-sensitive dyes. *J. Neurosci. Methods* **148:**94–102

Franzini-Armstrong, C., Ferguson, D.G., Champ, C. 1988. Discrimination between fast- and slow-twitch fibres of guinea pig skeletal muscle using the relative surface density of junctional transverse tubule membrane. *J. Muscle Res. Cell Motil.* **9:**403–414

Franzini-Armstrong, C., Protasi, F., Ramesh, V. 1998. Comparative ultrastructure of Ca^{2+} release units in skeletal and cardiac muscle. *Ann. N. Acad. Sci.* **853:**20–30

Fromherz, P., Lambacher, A. 1991. Spectra of voltage-sensitive fluorescence of styryl-dye in neuron membrane. *Biochim. Biophys. Acta* **1068:**149–156

Gonzalez-Serratos, H. 1971. Inward spread of activation in vertebrate muscle fibres. *J. Physiol.* **212:**771–799

Gross, E., Bedlack, R.S. Jr., Loew, L.M 1994. Dual-wavelength ratiometric fluorescence measurement of the membrane dipole potential. *Biophys. J.* **67:**208–216

Head, S.I. 1993. Membrane potential, resting calcium and calcium transients in isolated muscle fibres from normal and dystrophic mice. *J. Physiol.* **469:**11–19

Heiny, J.A., Ashcroft, P.M., Vergara, J. 1983. T-system optical signals associated with inward rectification in skeletal muscle. *Nature* **301:**164–166

Heiny, J.A., Vergara, J. 1982. Optical signals from surface and T system membranes in skeletal muscle fibers. Experiments with the potentiometric dye NK2367. *J Gen. Physiol.* **80:**203–230

Heiny, J.A., Vergara, J. 1984. Dichroic behavior of the absorbance signals from dyes NK2367 and WW375 in skeletal muscle fibers. *J. Gen. Physiol.* **84:**805–837

Hidalgo, C. 1985. Lipid phase of transverse tubule membranes from skeletal muscle. An electron paramagnetic resonance study. *Biophys. J.* **47:**757–764

Huxley, A.F., Taylor, R.E. 1958. Local activation of striated muscle fibers. *J. Physiol.* **144:**426–451

Kim, A.M., Vergara, J.L. 1998a. Fast voltage gating of Ca^{2+} release in frog skeletal muscle revealed by supercharging pulses. *J. Physiol.* **511:**509–518

Kim, A.M., Vergara, J.L. 1998b. Supercharging accelerates T-tubule membrane potential changes in voltage clamped frog skeletal muscle fibers. *Biophys. J.* **75:**2098–2116

Knisley, S.B., Justice, R.K., Kong, W., Johnson, P.L. 2000. Ratiometry of transmembrane voltage-sensitive fluorescent dye emission in hearts. *Am. J. Physiol.* **279:**H1421–H1433

Lannergren, J., Bruton, J.D., Westerblad, H. 1999. Vacuole formation in fatigued single muscle fibres from frog and mouse. *J. Muscle Res. Cell Motil* **20:**19–32

Nakajima, S., Gilai, A. 1980a. Action potentials of isolated single muscle fibers recorded by potential-sensitive dyes. *J. Gen. Physiol.* **76:**729–750

Nakajima, S., Gilai, A. 1980b. Radial propagation of muscle action potential along the tubular system examined by potential-sensitive dyes. *J. Gen. Physiol.* **76:**751–762

Obaid, A.L., Koyano, T., Lindstrom, J., Sakai, T., Salzberg, B.M. 1999. Spatiotemporal patterns of activity in an intact mammalian network with single-cell resolution: optical studies of nicotinic activity in an enteric plexus. *J. Neurosci.* **19:**3073–3093

Pediconi, M.F., Donoso, P., Hidalgo, C., Barrantes, F.J. 1987. Lipid composition of purified transverse tubule membranes isolated from amphibian skeletal muscle. *Biochim. Biophys. Acta* **921:**398–404

Revel, J.P. 1962. The sarcoplasmic reticulum of the bat cricothyroid muscle. *J. Cell Biol.* **12:**571–588

Rohr, S., Kucera, J.P. 1998. Optical recording system based on a fiber optic image conduit: assessment of microscopic activation patterns in cardiac tissue. *Biophys. J.* **75:**1062–1075

Rohr, S., Salzberg, B.M. 1994. Multiple site optical recording of transmembrane voltage (MSORTV) in patterned growth heart cell cultures: assessing electrical behavior, with microsecond resolution, on a cellular and subcellular scale. *Biophys. J.* **67:**1301–1315

Ross, W.N., Salzberg, B.M., Cohen, L.B., Grinvald, A., Davila, H.V., Waggoner, A.S., Wang, C.H. 1977. Changes in absorption, fluorescence, dichroism, and birefringence in stained giant axons: optical measurement of membrane potential. *J. Membrane Biol.* **33:**141–183

Salzberg, B.M., Davila, H.V., Cohen, L.B. 1973. Optical recording of impulses in individual neurones of an invertebrate central nervous system. *Nature* **246:**508–509

Squire, J.M. 1997. Architecture and function in the muscle sarcomere. *Curr. Opin. Struct. Biol.* **7:**247–257

Szentesi, P., Jacquemond, V., Kovacs, L., Csernoch, L. 1997. Intramembrane charge movement and sarcoplasmic calcium release in enzymatically isolated mammalian skeletal muscle fibres. *J. Physiol.* **505:**371–384

Tsau, Y., Wenner, P., O'Donovan, M.J., Cohen, L.B., Loew, L.M., Wuskell, J.P. 1996. Dye screening and signal-to-noise ratio for retrogradely transported voltage-sensitive dyes. *J. Neurosci. Methods* **70:**121–129

Tutdibi, O., Brinkmeier, H., Rudel, R., Fohr, K.J. 1999. Increased calcium entry into dystrophin-deficient muscle fibres of MDX and ADR-MDX mice is reduced by ion channel blockers. *J. Physiol.* **515:**859–868

Vergara, J., Bezanilla, F. 1976. Fluorescence changes during electrical activity in frog muscle stained with merocyanine. *Nature* **259:**684–686

Vergara, J., Delay, M. 1986. A transmission delay and the effect of temperature at the triadic junction of skeletal muscle. *Proc. R. Soc. Lond. B* **229:**97–110

Vergara J.L., Bezanilla F. 1981. Optical studies of E-C coupling with potentiometric dyes. In: A.G.M. Brazier, editor, The Regulation of Muscle Contraction: Excitation-contraction coupling. pp. 66–77. Academic Press, Inc., New York

Vergara J.L., Delay M., Heiny J.A., Ribalet B. 1983. Optical studies of T-system potential and calcium release in skeletal muscle fibers. In: A.G.a.W. Moody, editor, The Physiology of Excitable Cells. pp. 343–355. Alan R. Liss, Inc., New York

Woods, C.E., Novo, D., Difranco, M., Capote, J., Vergara, J.L. 2005. Propagation in the transverse tubular system and voltage dependence of calcium release in normal and mdx muscle fibres. *J. Physiol.* **568:**867–880

Woods, C.E., Novo, D., DiFranco, M., Vergara, J.L. 2004. The action potential-evoked sarcoplasmic reticulum calcium release is impaired in mdx mouse muscle fibres. *J. Physiol.* **557:**59–75

Zhang, J., Davidson, R.M., Wei, M.D., Loew, L.M. 1998. Membrane electric properties by combined patch clamp and fluorescence ratio imaging in single neurons. *Biophys. J.* **74:**48–53